Harnessing the Power of Repetition Structure in Ultra-Narrowband IoT

*Spyridon Peppas, *Paris A. Karakasis, *Nicholas D. Sidiropoulos, †Danijela Cabric
Department of ECE, *University of Virginia, Charlottesville, VA, U.S.A.
†University of California, Los Angeles, CA, U.S.A.
Email: {wxk3qj, pk4cf, nikos}@virginia.edu, danijela@ee.ucla.edu

***Abstract*—In this paper, we present a method for decoding uplink messages in Internet of Things (IoT) networks that employ packet repetition. We focus on the Sigfox protocol, but our approach is applicable to other IoT protocols that employ message repetition. Our approach endeavors to enhance the reliability of message capture as well as the error rate performance at the base station. To achieve this goal, we propose a novel technique that capitalizes on the unique features of the IoT network's uplink transmission structure. Through simulations, we demonstrate the effectiveness of our method in various scenarios, including single-user and multi-user setups. We establish the resilience of our approach under higher system loads and interference conditions, showcasing its potential to improve IoT network performance and reliability even when a large number of devices operates over limited spectrum. Our findings reveal the potential of the proposed method as a promising solution for enabling more dependable and energy-efficient communication in IoT Low Power Wide Area Networks.**

***Index Terms*—Generalized Canonical Correlation Analysis (GCCA), Random Access Protocols, Frequency-Hopping Spread Spectrum (FHSS), Internet of Things (IoT), SigFox.**

I. Introduction

The widespread deployment of IoT networks has led to an increasing demand for reliable and efficient communication protocols. Many of these protocols, such as SigFox, LoRa and NB-IoT, rely on the repetition of packets to ensure message delivery [1]–[4]. This redundancy, however, is not always exploited to its full potential, especially when the base station (BS) is equipped with multiple antennas. As the number of IoT devices grows, maximizing the benefits of this inherent redundancy becomes crucial for improving the performance of the overall network.

The primary objective of this paper is to address the following research question. How can the repetition structure of IoT protocols, as SigFox, be effectively utilized to improve the decoding process at a multi-antenna BS in order to enhance message reception reliability and overall network performance?

To achieve this objective, we propose a generalized Canonical Correlation Analysis (gCCA) based decoding method that leverages the inherent redundancy in the packet repetition structure while taking advantage of the spatial diversity offered by multiple antennas at the BS (Fig. 1). We demonstrate the efficacy of our method through simulations for single and multiple users, highlighting its potential impact on the reliability of IoT networks.

This research work was supported partially by NSF ECCS-2118002 and AST-2132700.

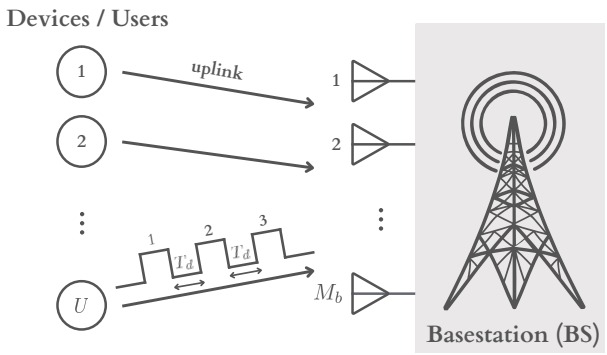

Fig. 1. SigFox uplink communication.

The main contributions of this work are as follows.

- Demonstrating the effectiveness of the proposed gCCA-based method in both single and multiple user scenarios.
- Establishing that the gCCA method enables more reliable and energy-efficient communication in IoT LPWAN.
- Highlighting the robustness of gCCA in the face of interference, which underpins the improvement of performance and dependability in IoT networks even when multiple IoT devices share the same wireless medium.

In order to build upon these foundational concepts, we first discuss the main features of SigFox and similarities with other IoT protocols, and highlight the importance of exploiting packet repetition for enhanced network performance.

II. System Model

A. SigFox Technology Overview

SigFox is an ultra-narrowband IoT communication technology that operates at the 868 MHz frequency band in Europe and the 915 MHz band in the United States. In Europe, it supports a physical layer data rate of 100 bps for a 100 Hz bandwidth and 1000 bps for a 1 kHz bandwidth, while in the United States it offers a data rate of 600 bps, which corresponds to a bandwidth of approximately 600 Hz [5]. Sigfox devices are capable of transmitting up to 140 messages per day to a base station (uplink, Fig. 1). Each message has a maximum packet length of 24 bytes (192 DBPSK symbols),

which includes a 32-bit preamble and 16-bit CRC (Cyclic Redundancy Check) frame [4]–[6].

SigFox enhances communication reliability through message repetitions and frequency hopping, sending three copies of a message across various frequencies to avoid interference and ensure high reception rates. This, along with frequency hopping between messages, reduces collision risks and strengthens network resilience. These strategies are crucial for SigFox's success in providing efficient, reliable connectivity for IoT applications requiring long-range communication and durability.

B. Signal Model

During the Medium Access Control (MAC) layer transmission of SigFox, a device encapsulates its data within a packet and sends it three times with specific, and identical across all devices, time delays, T_d, using three different random hopping frequencies [5]–[7]. Given the low data rate, R, the transmitted signal occupies a relatively narrow instantaneous bandwidth W. Frequency hopping occurs within a bandwidth $B \gg W$, which offers channel diversity for protection against deep fading and occasional collisions.

The baseband signal (packet) generated by each device or user u is expressed as [7]

$$x_u(t) = \sum_{k \in \mathcal{S}} a_k^{(u)} \phi\left(t - kT\right), \tag{1}$$

where T denotes the symbol period, $\phi(t)$ refers to the pulse shaping filter with a bandwidth of W, $\mathcal{S}$ denotes the set of symbols within the packet, and $a_k^{(u)}$ indicates the symbol of the u-th user transmitted at time kT. Although SigFox primarily uses Differential-Binary-Phase-Shift-Keying (DBPSK), other constellations like Symmetric-Binary-Phase-Shift-Keying (SBPSK), 4QAM, 8PSK, and 16QAM can be adopted. Each transmitted signal, across different users and repetitions, can be described as follows

$$\begin{aligned} &z_{r,u}(t) = x_u(t)\, e^{j2\pi df_{r,u} t}, \\ &r \in \{1,2,3\},\ u \in \{1,2,\ldots,U\}. \end{aligned} \tag{2}$$

In this expression, r represents the r-th repetition of the u-th user's signal, df denotes the frequency hopping including the center frequency and any carrier frequency offset (CFO).

When transmissions of different users (IoT devices) overlap in time, each of the M_b antennas at the BS receives a linear combination of delayed versions of the transmitted signals. More specifically, in the case of a maximal number of users, $U_{\max}$, and in the presence of additive white circularly symmetric Gaussian noise of variance, σ_w^2, the received signal at the m-th antenna can be described as

$$\begin{aligned} y^{(m)}(t) = \sum_{u=1}^{U_{\max}} \sum_{r=1}^{3} h_{r,u}^{(m)}\ z_{r,u}\left(t - rT_d - T_a^{(u)}\right) + w^{(m)}(t), \\ w^{(m)}(t) \sim \mathcal{CN}\left(0, \sigma_w^2\right), \\ m \in \{1,2,\ldots,M_b\}, \end{aligned} \tag{3}$$

where $h_{r,u}^{(m)}$ denotes the flat fading channel of the r-th repetition of the u-th users' transmission at the m-th antenna of the BS, while $T_a^{(u)}$ denotes the asynchronous delay linked to the u-th user and determines the beginning of their transmission.

To effectively analyze the communication system's performance, it is essential to consider not only the signal model but also the impact of the channel on the transmitted signal. In the following section, we will introduce a suitable channel model that takes into account the fading characteristics of the wireless medium.

C. Channel Model

The Rician model is particularly useful in scenarios where a strong path exists due to direct line-of-sight (LoS) between the transmitter and receiver [8]. The Rician model can be formulated as

$$h = \sqrt{\frac{k_h}{k_h+1}}\sigma_h e^{j\theta} + \sqrt{\frac{1}{k_h+1}}\ \mathcal{CN}\left(0, \sigma_h^2\right),\ \theta \sim \mathcal{U}[0, 2\pi).$$

In the Rician model, the first term represents the contribution of the LoS path, which has a deterministic component, while the second term accounts for the contribution of the remaining paths. The parameter k_h is the ratio between the power of the LoS path and the power of the remaining paths. As a result, a larger ratio results in a more deterministic channel. In general, random variable $|h|$ follows the Rice distribution. However, when $k_h = 0$, the Rician fading reduces to the Rayleigh one. Furthermore, using the confluent hypergeometric function, it can be deduced that $\mathcal{E}\{|h|^2\} \equiv \sigma_h^2$ based on the Nakagami n-distribution [9].

Integrating the signal and channel models offers a holistic approach for examining and evaluating the communication system. By combining these models, we can delve into multiple aspects, including frequency hopping, channel fading, and multi-user interference, in order to assess the overall system performance.

III. Signal Detection via generalized CCA

Under the assumption that the receiver is cognizant of the delay T_d between repetitions and the hopping frequencies, it is possible to apply matched filtering to segments of $y^{(m)}(t)$ that correspond to a given user. Assuming perfect synchronization for the detection of the first symbol, this approach results in collecting symbol-spaced sequences, $\mathbf{y}_r^{(m)} \in \mathbb{C}^{N\times 1}$, at each antenna m of the BS, which correspond to the r-th repetition of a user. Given $r = 3$, three distinct views of the signal can be written out as follows

$$\mathbf{Y}_r = \left[\mathbf{y}_r^{(1)}, \mathbf{y}_r^{(2)}, \ldots, \mathbf{y}_r^{(M_b)}\right] \in \mathbb{C}^{N\times M_b},\ r \in \{1,2,3\}, \tag{4}$$

where N represents the number of transmitted symbols.

If we deal with a single user situation, the collected views would share a common subspace of dimension 1, determined by scaled versions of the users' symbols, in the absence of additive noise. Consequently, gCCA can be employed to

extract a basis of the common subspace (component in our 1d case) [10]

$$\min_{\mathbf{g},\{\mathbf{q}_r\}_{r=1}^3} \sum_{r=1}^{3} \|\mathbf{Y}_r\mathbf{q}_r - \mathbf{g}\|_2^2 \quad \text{s.t.} \quad \|\mathbf{g}\|_2^2 = 1. \tag{5}$$

Eq. (5) represents the MAX-VAR formulation of gCCA. Its goal is to find the common component, $\mathbf{g} \in \mathbb{C}^{N\times 1}$, up to scaling[1], via specifying the reducing operators $\mathbf{q}_r \in \mathbb{C}^{M_b\times 1}$, for $r \in \{1,2,3\}$. Recent work in [11] has demonstrated that the sought user packet can be reliably recovered even if it is subject to strong interference – provided that the latter does not repeat in a synchronous fashion.

After letting, $\mathbf{Y}_r = \mathbf{U}_r\mathbf{\Sigma}_r\mathbf{V}_r^{\mathcal{H}}$, $\mathbf{U}_r \in \mathbb{C}^{N\times M_b}$ denote the Singular Value Decomposition (SVD) of matrices $\mathbf{Y}_r$, $r \in \{1,2,3\}$ respectively, it can be shown that the problem (5) can be expressed only in terms of vector $\mathbf{g}$ as

$$\max_{\mathbf{g}} \ \mathbf{g}^{\mathcal{H}}\left(\sum_{r=1}^{3}\mathbf{U}_r\mathbf{U}_r^{\mathcal{H}}\right)\mathbf{g} = \left\|\mathbf{g}^{\mathcal{H}}\underbrace{[\mathbf{U}_1,\ \mathbf{U}_2,\ \mathbf{U}_3]}_{\mathbf{M}}\right\|_2^2 \quad \text{s.t.} \quad \|\mathbf{g}\|_2^2 = 1, \tag{6}$$

where the Hermitian operation is denoted by $(\cdot)^{\mathcal{H}}$. This yields a principal component problem, namely finding the left principal singular vector of the matrix $\mathbf{M} \in \mathbb{C}^{N\times 3M_b}$, which can be achieved via truncated SVD. The overall complexity for forming matrix $\mathbf{M}$ and solving problem (6) is upper bounded by the complexity of computing the SVD of matrix $\mathbf{M}$, which is $\mathcal{O}\left(NM_b^2\right)$ and hence linear in N.

Up to this point, we have assumed that we have a single user with known timing and hop sequence, yielding a common subspace of dimension one. In multiuser scenarios such as Sigfox, the situation is more challenging and requires careful treatment, as we will see in the sequel.

A. Frequency Detection

As in SigFox and related IoT protocols, we divide the overall bandwidth B into smaller sub-bands of bandwidth W and dwell (subcarrier) frequencies that form a frequency grid, denoted by $\boldsymbol{f}_{\text{grid}}$. In our prior analysis, we assumed that the receiver has knowledge of the hopping frequencies, enabling it to lock on to a specific user packet. In practice, this information is not available at the BS, because of the large number of devices it serves and the desire to support drop-and-play functionality without handshake and with intermittent transmission patterns. Consequently, it becomes crucial to identify the frequencies associated with a specific user at a given time.

The frequency detection problem can be separated into three distinct sub-problems. First, the frequency pair corresponding to $\mathbf{Y}_1$ and $\mathbf{Y}_3$ has to be identified, followed by determining the frequency pair related to $\mathbf{Y}_1$ and $\mathbf{Y}_2$. This procedure entails performing matched filtering across multiple frequency pairs, solving problem (5) for every pair of views, and evaluating their cost functions to identify the best-matching pairs. After finding the optimal frequency hops from these two sub-problems, a final gCCA problem incorporating $\mathbf{Y}_1$, $\mathbf{Y}_2$, and $\mathbf{Y}_3$ is solved to obtain the symbols from the common component $\mathbf{g}$. Note that transmitter-specific CFO may persist, due to transmitter-receiver oscillator mismatch, especially of low-cost IoT devices. A simple method can be employed to estimate and correct this residual CFO after down-conversion, using the FFT of the signal raised to a suitable constellation-dependent power to eliminate the dependence on the transmitted symbols; see [12].

[1]We can re-scale our symbols back to the constellation by utilizing the preamble.

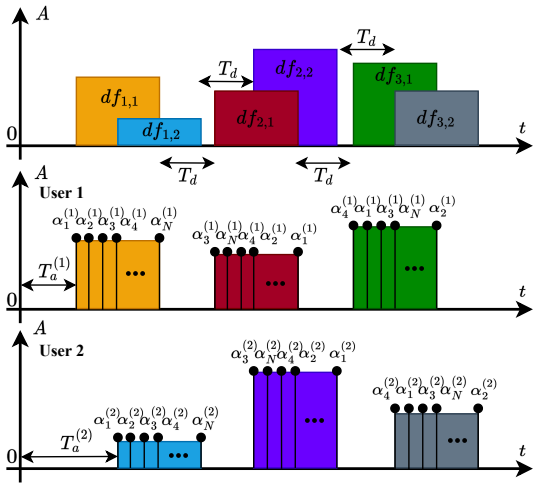

Fig. 2. Example of two users colliding in time domain, and shuffling of repetition 2 and 3. Different colors denote different hop frequency bins, while the varying heights of the different transmission blocks illustrate the effects of time-selective fading. There are no frequency collisions in this figure, for clarity of illustration. The common reshuffling of the symbols during retransmissions is also depicted, and is used to break the repetition structure in time-misaligned interference.

B. Challenges when multiple co-channel users hop and repeat

Earlier work [10], [11] had considered a scenario where an underlay user is potentially "buried" under a primary user. The underlay user repeats (without frequency hopping), but the primary user does not. The latter assumption is crucial for correct recovery of the underlay user. In our present context, the situation is more intricate. Multiple peers hop and repeat, creating potential collisions in time and frequency, possibly inducing a common subspace of dimension higher than one.

Fig. 2 showcases an example where two users' transmissions have partial overlap in the time domain. If two replicas among two users exhibit extensive time overlap and their frequency hops collide, the common subspace has dimension two, as the delay T_d between repetitions is the same for all the users[2]. If we utilize CCA to find the best frequency pair for a common subspace of dimension 1, frequency matching will fail.

To tackle this issue and guarantee a one-dimensional common subspace, we bring in a simple modification to the trans-

[2]Otherwise time synchronization would be a much more challenging task.

mitter line code. The proposed modification effectively breaks the repetition structure of time-misaligned interference, even when it hits on the same pair of frequency hops. Specifically, each user sends their first replica unchanged, while the second and third replicas are shuffled using two interleavers which are common to all users – see Fig. 2. Note that the interleavers can be pre-programmed from the factory. They are neither user device-specific nor BS-specific, thus supporting drop-and-play deployment. This enables the receiver to employ the same de-interleaving technique for every user without the need to explore different shuffling codes. By adopting this strategy, we successfully create unique interference patterns among all repetitions, ensuring a common subspace of dimension one even when users experience persistent frequency overlap – as long as they are not also perfectly aligned in time.

C. Overall Time Complexity

At first glance, our method may appear to be time-consuming due to the necessity of solving a series of gCCA problems to determine frequency pairs and produce a final estimate based on gCCA. When $\boldsymbol{f}_{\text{grid}}$ comprises N_f hop frequencies, the overall complexity of our algorithm becomes $\mathcal{O}(NM_b^2N_f^2)$. However, it is not imperative to scrutinize every frequency in the grid, but only those frequency bins that have energy content exceeding a certain threshold, indicating the presence of a packet. By adopting this strategy, the complexity becomes $\mathcal{O}(NM_b^2U_{\text{act}}^2)$, where U_{act} is the number of simultaneously active users, which is $\leq U_{\max}$.

IV. Numerical Results

In this section, we will evaluate the efficiency of the gCCA-based method through a series of Monte Carlo experiments. To assess the performance of our approach, we define the signal-to-noise ratio (SNR) as

$$\mathsf{SNR}_{\text{dB}} = 10\log_{10}\left(\frac{\sigma_h^2}{T_s\sigma_w^2}\right), \tag{7}$$

where, T_s is the sampling period. By specifying the SNR in this manner, we model the signal-to-noise ratio at the output stage of the pulse-shaping filter of the receiver, maintaining it at the predetermined SNR_{dB} level[3]. One way to control the SNR in our Monte-Carlo experiments is to fix the power of noise and set the power of the channel, accordingly.

For comparison purposes, we consider the following baseline method (B.line), which uses the preamble symbols for channel estimation and employs Maximum Ratio Combining (MRC) to benefit from the multi-antenna diversity. Moreover, B.line exploits the frequency diversity afforded by multi-hop transmission in the SigFox protocol, without however fully harnessing this repetition structure. It only decodes one hop at a time, trying out each frequency bin in turn and checking if the decoded packet passes CRC check. We also apply the CRC-check to our method after correcting the scaling of g

[3]Eq. (7) is accurate under the condition that the power of the transmitted symbols, considered as random variables, is equal to 1.

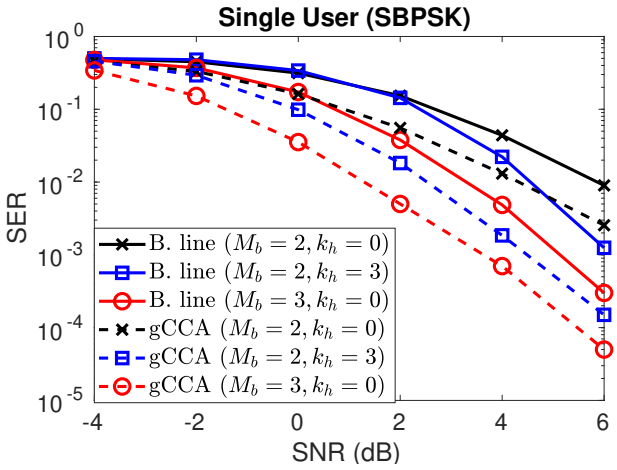

Fig. 3. Single user: SNR vs SER for different fading parameters and varying number of antennas at the BS.

using the preamble. In cases where the CRC-check fails, we set the corresponding error rate to 0.5 (coin flip).

In order to simplify the comparison of the proposed and the B.line method, we assume ideal time synchronization at the receiver, which means that we do not need to search for the first replica's starting point. Given that we presume knowledge of the starting points, there is no requirement for identification and routing, making the Frame Sync. and MAC Header components of the SigFox frame structure [5], [6] unnecessary for these simulations. Consequently, apart from the preamble and CRC, the rest of the packet is treated as payload. Additionally, although CFO is not considered in our experiments, it can be readily accommodated using the FFT method described earlier in Section III-A.

Unless otherwise stated, the noise power σ_w^2 is set to -90 dBm. The pulse shaping function selected is the squared-root-raised-cosine (SRRC) with roll-of-factor $a = 0.5$ and symbol period $T = 1.5$ msec – this ensures that the bandwidth of the transmitted packet occupies $W = 1$kHz. The sampling period, T_s, is defined as $T_s \triangleq \frac{T}{\text{over}}$, where 'over' represents the oversampling parameter. Furthermore, the total number of transmitted symbols, N, is set to 192 from an SBPSK constellation ($\{0,1\} \to \{0-1j, 0+1j\}$), with the initial 32 symbols serving as the preamble. Moreover, CRC-16-Kermit-0x1021 is utilized as the checksum algorithm due to its well-established error detection capabilities. The performance evaluation of the methods is conducted using the Symbol Error Rate (SER). The oversampling factor is set to 12, while $\boldsymbol{f}_{\text{grid}}$ contains 8 distinct hopping frequencies.

In the first experiment, we examined a single-user setup (corresponding to a lightly loaded system where collisions are very rare) with $M_b \in \{2,3\}$ antennas at the BS, and varying fading parameters $k_h \in \{0,3\}$. We performed 10^4 Monte Carlo experiments for each choice of system parameters. As evidenced by Fig. 3, we can confidently assert that our proposed gCCA method surpasses the B.line method for all cases under identical system parametrization. Specifically, both methods (B.line and gCCA) benefit from improved fading at $k_h = 3$ compared to $k_h = 0$, which represents the worst-case

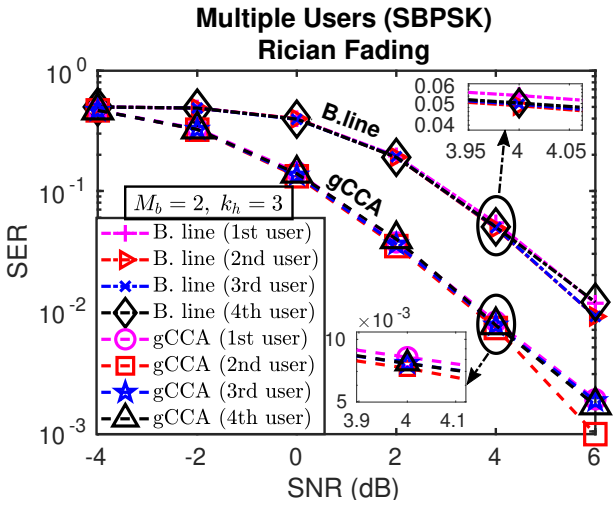

Fig. 4. Multiple users: SNR vs SER for $M_b = 2$ and $k_h = 3$.

Rayleigh scenario. The gCCA method demonstrates an improved performance by 2dB in terms of SNR when $\mathrm{SNR} > 0$. Furthermore, when the antenna count is raised to $M_b = 3$, it becomes evident that our proposed method more effectively exploits the increased number of antennas at the BS, particularly at lower SNR values ($\mathrm{SNR} \leq 0$). This difference is more pronounced compared to the B.line method when using three antennas as well. Although we employed a simple SBPSK constellation to adhere more closely to the SigFox protocol standard, our method can still deliver high performance when using higher-order constellations, thus providing better data rates. In contrast, a basic channel estimation method would likely falter in such cases. However, the single-user scenario is relatively straightforward, and associated gains are relatively limited. The real challenge arises when handling multiple users and a congested medium, which can result in persistent time and frequency collisions.

In light of this, we conducted a second experiment with four interfering users. We let the user delays $T_a^{(u)}$ (expressed in samples) be independent and uniformly distributed random variables in $\{0, 250, 500, 750, 1000, 1250, 1500, 1750\}$. The intra-hop delay T_d is fixed at 1750 samples, so there is always partial or complete time overlap between the users, since the packet length is 2400 samples. The eight available hop frequencies are also drawn in an i.i.d. fashion across users and repetition. Thus, the single-hop collision probability equals the frequency collision probability, which is $1 - \left(\frac{7}{8}\right)^3 \approx 0.33$. As mentioned in section III-A, our method will operate effectively in such setting if we interleave the second and third repetitions' symbols prior to transmission. Consequently, we randomly shuffle the symbols for these replicas in an identical manner for all users, allowing the receiver to seamlessly de-interleave them.

Fig. 4 displays the SER as a function of SNR for each user employing the baseline and our proposed approach, after performing 10^4 Monte Carlo experiments when $k_h = 3$, $M_b = 2$. We incorporated this fading to sustain balanced interference among all repetitions, a circumstance that is most challenging from a packet capture point of view.

Although SINR is not explicitly depicted on the x-axis, it is important to consider that users only interfere when colliding in both time and frequency domains. For scenarios where four users collide simultaneously on the same frequency and time, the SINR for a single transmission could be less than -6 dB, when $\mathrm{SNR} = 2$ dB. However, this value may vary depending on fading and environmental factors.

The situation may seem extraordinary, involving only eight frequencies for hopping, yet it is crucial to acknowledge that in real-life scenarios, there could be up to thousands of users/devices competing for spectrum. Observing Fig. 4, the proposed method demonstrates a performance improvement in the order of 3 dB in terms of SNR. Hence, the proposed approach supports reliable communication at lower SNRs, unlike the baseline, which is important for extending the range and battery life of power-limited IoT devices in real-world applications. It is also important to mention that our approach can naturally tolerate strong broadband interference from other unlicensed (non-IoT) sources, such as industrial emissions, which is something that the baseline method cannot do.

V. Conclusions

Our work has successfully demonstrated the efficacy of the proposed gCCA-based method for reliable detection in low power IoT devices, specifically focusing on the SigFox protocol, but also applicable to other IoT protocols that use repetition and frequency hopping to mitigate fading and multiuser interference by other IoT devices. By exploiting the narrowband and repetitive nature of such IoT standards, we have developed a technique that significantly improves the performance of these systems. Through simulations, we have shown that gCCA outperforms the baseline approach under varying fading conditions and antenna configurations, delivering more reliable and energy-efficient communication in IoT LPWAN. These advancements contribute to enhancing the performance and reliability of IoT networks when encountering devices coexisting on the same wireless medium.

References

[1] C. Goursaud and J.-M. Gorce, "Dedicated networks for IoT : PHY / MAC state of the art and challenges," *EAI endorsed transactions on Internet of Things*, Oct. 2015.

[2] H. Mroue, A. Nasser, S. Hamrioui, B. Parrein, E. Motta-Cruz, and G. Rouyer, "MAC layer-based evaluation of IoT technologies: LoRa, SigFox and NB-IoT," in *2018 IEEE Middle East and North Africa Commun. Conference (MENACOMM)*, Apr. 2018, pp. 1–5.

[3] M. Centenaro, L. Vangelista, A. Zanella, and M. Zorzi, "Long-range communications in unlicensed bands: the rising stars in the IoT and smart city scenarios," *IEEE Wireless Communications*, vol. 23, no. 5, pp. 60–67, Oct. 2016.

[4] A. Khalifeh, K. A. Aldahdouh, K. A. Darabkh, and W. Al-Sit, "A Survey of 5G Emerging Wireless Technologies Featuring LoRaWAN, Sigfox, NB-IoT and LTE-M," in *International Conference on Wireless Commun. Signal Proc. and Networking (WiSPNET)*, 2019, pp. 561–566.

[5] E. Morin, M. Maman, R. Guizzetti, and A. Duda, "Comparison of the Device Lifetime in Wireless Networks for the Internet of Things," *IEEE Access*, vol. 5, pp. 7097–7114, 2017.

[6] S. Build, "Sigfox connected objects: Radio specifications," Mar. 2022.

[7] G. Ferré and E. P. Simon, "An introduction to Sigfox and LoRa PHY and MAC layers," Apr. 2018. [Online]. Available: https://hal.science/hal-01774080

[8] A. Goldsmith, *Wireless Communications*. USA: Cambridge University Press, 2005.

[9] M. Nakagami, "The m-Distribution—A General Formula of Intensity Distribution of Rapid Fading," in *Statistical Methods in Radio Wave Propagation*. Pergamon, 1960, pp. 3–36.

[10] M. S. Ibrahim, P. A. Karakasis, and N. D. Sidiropoulos, "A Simple and Practical Underlay Scheme for Short-range Secondary Communication," *IEEE Trans. Wireless Commun.*, pp. 1–1, Jun. 2022.

[11] M. S. Ibrahim and N. D. Sidiropoulos, "Blind Carbon Copy on Dirty Paper: Seamless Spectrum Underlay via Canonical Correlation Analysis," in *"Proc. IEEE Int. Conf. Acoust. Speech Signal Process. (ICASSP)"*, 2021, pp. 8123–8127.

[12] A. M. Wyglinski, R. Getz, T. Collins, and D. Pu, *Software-defined radio for engineers*. Artech House, 2018.